

Article

A Multi-Function Conversion Technique for Vehicle-to-Grid Applications

Ying Fan ^{1,*}, Weixia Zhu ^{1,†}, Zhongbing Xue ^{2,†}, Li Zhang ^{1,†} and Zhixiang Zou ^{3,†}

¹ School of Electrical Engineering, Southeast University, Nanjing 210096, Jiangsu, China; E-Mails: Zhuwx19910114@163.com (W.Z.); zhangli_870816@163.com (L.Z.)

² Yangzhou Electric Power Corp., Yangzhou 225012, Jiangsu, China; E-Mail: zbxue2313@163.com

³ Chair of Power Electronics, Christian-Albrechts-Universität zu Kiel, Kiel 24143, Germany; E-Mail: zou.zhixiang@163.com

† These authors contributed equally to this work.

* Author to whom correspondence should be addressed; E-Mail: vickifan@seu.edu.cn; Tel./Fax: +86-25-8379-4152.

Academic Editor: Joeri Van Mierlo

Received: 11 May 2015 / Accepted: 21 July 2015 / Published: 27 July 2015

Abstract: This paper presents a new multi-function conversion technique for vehicle-to-grid (V2G) applications. The proposed bi-directional charger can achieve three functions, including EV battery charging, grid-connection and reactive compensation, which are keys for energy management of the grid. With the proposed multi-function technology, the bi-directional charger will benefit both the grid and electricity customers. A hybrid regulation of energy bi-directional transfer for V2G systems is proposed in this paper, which consists of the battery-side controller and the grid-side controller. This proposed multi-function conversion technique improves the whole system performance with proportional-resonant (PR) control and achieves reactive power compensation with instantaneous reactive theory and a deadbeat control scheme. Simulation and experimental results demonstrate the validity of this new multi-function technique in a V2G system.

Keywords: electric vehicle; PR; reactive compensation; smart grid; V2G

1. Introduction

Due to the increasingly prominent energy problem and environmental pollution, electric vehicles (EVs) are gradually replacing traditional automobiles equipped with internal combustion engines. Meanwhile, the continuous development of outstanding performance batteries and high-efficiency motors also has spurred dramatic interest in EVs, which are regarded as representatives of new energy vehicles [1–4]. In addition, with the emergence and development of the concept of smart grid, the reliable, economic, efficient and clean performance of smart grid and its user-friendly interaction will give EVs brighter prospects and a new round of improvements [5–7]. Therefore, V2G technology, the product of interaction between the smart grid and EVs, will become more and more attractive. Figure 1 represents a basic V2G framework which consists of general grid elements, renewable energies, loads and some other smart systems [8,9]. According to the V2G concept, EVs are not only traditional power consumers, but also mobile distributed generators (DGs) returning the extra power to the grid when they are idle, which can improve energy management of the grid [10–12]. On the other hand, it is generally known that the reactive compensation plays an important role in improving the power quality and providing the grid with an economical and efficient operating mode [13]. Realizing the local compensation of reactive power with less investment and quicker effect is important to the power system. Considering the large scale applications of EVs and the advantages of V2G system, such as fast response and no additional cost, EVs are the promising devices for reactive power local compensation.

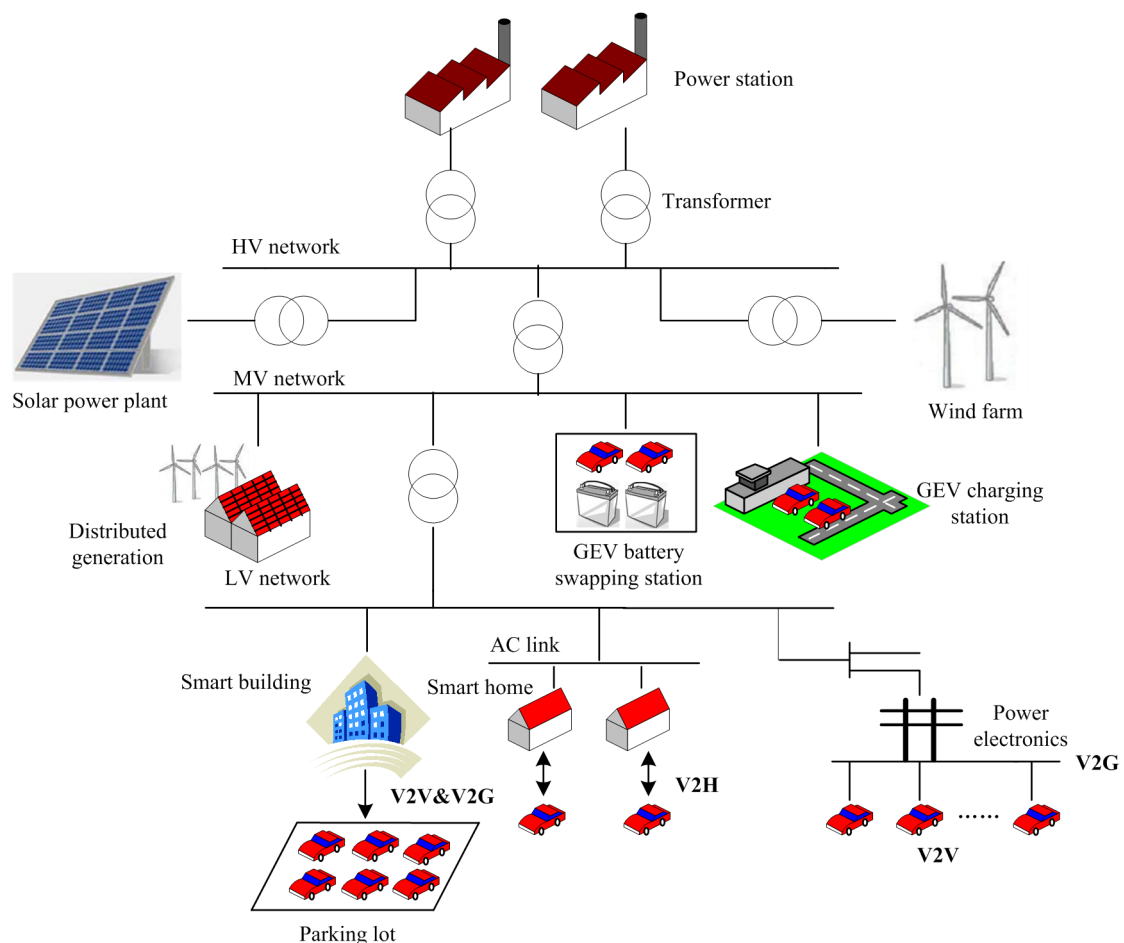


Figure 1. Framework for V2G.

As EVs' core component and technology, the power battery and its management technology must be taken seriously. Three main kinds of batteries used in EVs, such as lead-acid, nickel-hydrogen and lithium-ion batteries, are focused on in [3]. Meanwhile, some detailed comparative analysis of the technical and economic aspects of EV batteries' chemistry performance and application has been carried out. Different characteristics of the batteries make the energy vary. Two fast techniques which can be used to measure the state of health of a lithium-ion battery were introduced in the V2G application area [4]. A bidirectional converter topology for a V2G system is discussed in [14]. It offers advantages in power density, size, cost, efficiency, power quality, and so on. A new and attractive Z-Source inverter is introduced in [15] for the power electronics interface. The equivalent DC-link voltage ripple of the Z-Source inverter is analyzed. The theoretical findings and design rules are confirmed by simulation and experiment. In reference [16], an AC/DC matrix converter topology is presented and an optimized modulation strategy is proposed to reduce the charging current ripple. It can operate in two charging modes: constant voltage charging and constant current charging. In the references above, several circuit topologies and control methods are discussed and the advantages of each are analyzed correspondingly, but all they show are the topologies' optimal design and analysis focused on the operating modes of charging and discharging for EVs.

A globally optimal scheduling scheme and a locally optimal scheduling scheme for EV charging and discharging are proposed in [17]. Paper [18] presents an interaction protocol among the power grid, Energy Storage (ES), and EVs. It also demonstrates how to integrate the proposed scheduling approach to achieve real-time charging operations. A decentralized V2G control method for EVs is proposed in [19]. It participates in primary frequency control considering charging demands from EV customers. In reference [20], an extended standard is proposed by defining the information model for controlling the charging and discharging of EVs. However, the above methods just tackle a few issues such as charging, discharging and the interaction information. What's more, the function of reactive power compensation hasn't been implemented.

An improved multi-functional energy recovery power accumulator battery pack testing system for EVs is proposed in [21]. It has the functions of harmonic detection, suppression, reactive compensation and energy recovery. The study in [22] illustrates the effect of reactive power transfer on the V2G charger components through relating the AC and DC side variables. However, the analysis of the DC-DC converter and battery for reactive power support still needs to be studied in the future. In [23], the papers investigate the feasibility of supplying reactive power by V2G. They also analyze the hysteresis current controller of a single-phase inverter for V2G reactive power compensation. Nevertheless, the strategies which are used to realize the reactive power compensation and the relevant experimental verification are rarely analyzed, therefore, it is necessary to develop a new method for V2G to achieve a multi-function conversion technique which includes EV battery charging, grid-connection and local reactive compensation.

The major contribution of this paper is to propose a multi-function conversion technology for V2G, including EV battery charging, grid-connection and reactive compensation. Compared with the traditional V2G power transfer technology, the multi-function EV system proposed in this paper can operate in different modes and realize local reactive compensation. An integrated control strategy of energy bi-directional transformation for the V2G system, which consists of a battery-side controller and a grid-side controller, is studied. To improve the control effect, grid voltage feed-forward control and

PR control are introduced and analyzed. Furthermore, to achieve local reactive power compensation, the corresponding control schemes combined with instantaneous reactive power detection methods and deadbeat control are implemented. Moreover, the protection unit is employed to reinforce the reliability of the whole system. This paper is organized as follows: the bi-directional EV system is discussed in Section 2. The proposed control strategy for both the battery-side and the grid-connected converters is presented and a flexible control scheme for reactive power compensation is also investigated. In Sections 3 and 4, the simulation and experimental verifications are given and finally the conclusions are drawn in Section 5.

2. Results and Discussion

2.1. System Description

Based on the Chinese household electric system, the proposed bi-directional transfer circuit topology for V2G is put forward in Figure 2, which includes a grid-side converter, a protection circuit and a battery-side converter. Meanwhile, this V2G system can operate in three modes: charging mode, grid-connected mode and reactive power compensation mode.

In different operating modes, even if it is the same part of this proposed circuit, the circuit elements will play a different role. In charging mode, the grid-side converter is a PWM rectifier and the battery-side converter is a buck converter. In grid-connected mode, the grid-side converter is a PWM inverter and the battery-side converter is a boost converter. In reactive power compensation mode, the grid-side converter is a reactive power compensator and the battery-side converter is a boost converter. The protection circuit is designed to provide a discharging channel, which can consume surplus energy on the circuit and thus limit the voltage value of the DC-link.

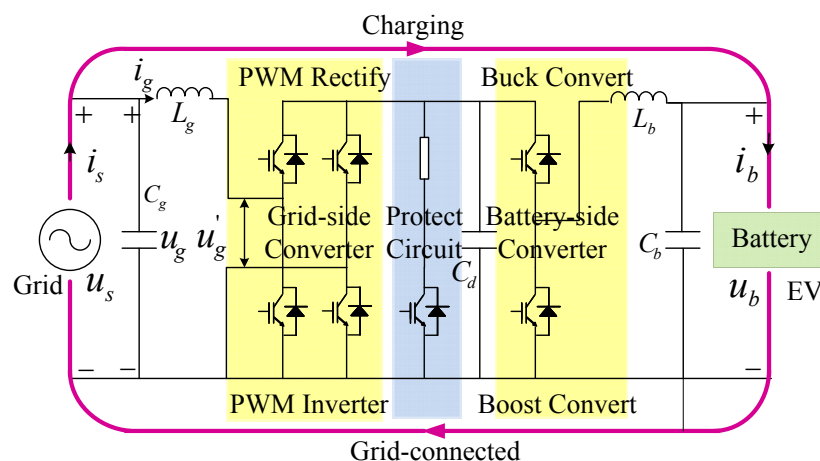


Figure 2. The proposed bi-directional transfer circuit topology for V2G.

2.2. Proposed Control Strategy

2.2.1. The Control Scheme of the Battery-Side Converter

According to the charging and discharging characteristics of the power cell, the battery voltage is very low during the initial stage of charging. Therefore, the constant current (CC) charging mode is

employed at the initial stage for extending battery life. In order to maintain the terminal voltage of the battery, the constant voltage (CV) charging mode is used when the output voltage reaches the rated value. As the charging process continues, the charging current is gradually decreasing. When the charging current is below the threshold which does not affect the battery life, a trickle current charging mode is in service to maintain a low current charge till the charging process completes.

Therefore, a control scheme aiming at maintaining constant voltage and regulating charging current is proposed. Based on the analysis of the proposed V2G topology, the battery-side converter should provide the constant current charging mode during the initial stage and the trickle current charging mode later. Furthermore, when the EVs are grid-connected, a DC-link voltage feedback controller is included to ensure that the DC bus voltage is greater than the peak value of the AC grid voltage. The block diagram of the whole battery-side control system is illustrated in Figure 3.

For the battery-side bidirectional DC-DC converter, the process of battery charging and discharging is the buck or boost transformation process of the circuit. Hysteresis or PWM modulation can be used to generate the duty cycle of the converters.

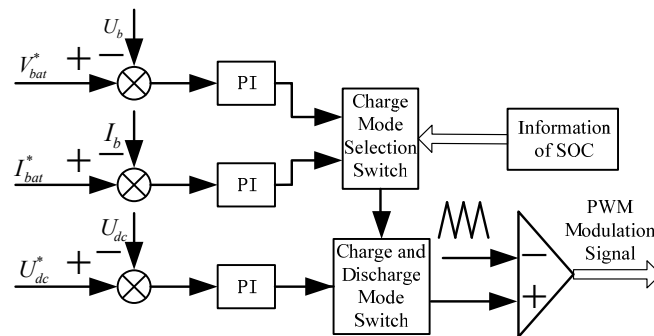


Figure 3. The control strategy block diagram of battery-side converter.

As shown in Figure 3, the charging or discharging state depends on the charge and discharge mode switch. When the battery is charging, the charge mode is automatically selected according to the battery state of charge (SOC). When the battery is discharging (the EV is grid-connected), it only needs to keep the bus voltage output constant.

2.2.2. The Control Scheme of Grid-Side Converter

The improved V-I double-loop control scheme is employed in the grid-side converter control which is shown in Figure 4.

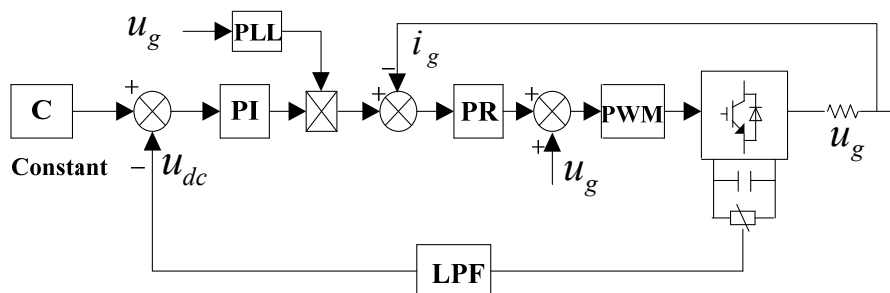


Figure 4. The improved bi-directional DC-AC control strategy of grid-side converter.

In different operating modes, the corresponding control strategy of the grid-side inverter will be different. In charging mode, the grid-side current is regulated by a PR controller to eliminate steady-state errors. Moreover, a voltage feed-forward is used to enhance the dynamic performance, restrain the variation of grid voltage and reduce the tracking errors of the system. These PWM signals with PR controller are introduced to control the converter which is performed in rectifier mode.

In the grid-connected mode, to achieve zero steady-state errors, a PR controller has more advantages in a stationary frame than a PI controller with infinite gain at the resonant frequency and preferable reference tracking capability. Therefore, a PR controller is also employed instead of a PI controller in this mode so the improved control strategy of the grid-side converter achieves bi-directional DC-AC transformation through introducing a revised inner current loop. The PR controller is defined as follows:

$$G_c(s) = K_p + K_i \times \frac{2\omega_c s}{s^2 + 2\omega_c s + \omega_0^2} \tag{1}$$

where K_p is the proportional coefficient, determining the dynamic response of the system; K_i is the resonant coefficient, adjusting the phase shift between the output and the reference; ω_c is the cutoff frequency; and ω_0 is the resonant frequency.

A low-pass filter (LPF) is introduced to eliminate the oscillations of the DC-link voltage. The PR control can achieve zero steady-state error in the stationary frame because of the large gain at the selected frequency.

2.3. Control Strategy for Reactive Power Compensation

A simplified model for the household single-phase power supply system is shown in Figure 5, where the power grid is considered to be infinite and all the loads and EVs are the terminal loads. In Figure 5, $i_s = i_g + i_L$ and $u_s = u_g = u_L$, where u_s and i_s are grid-side voltage and current respectively; u_L and i_L are load-side voltage and current; and u_g and i_g are the voltage and current of grid-side converter.

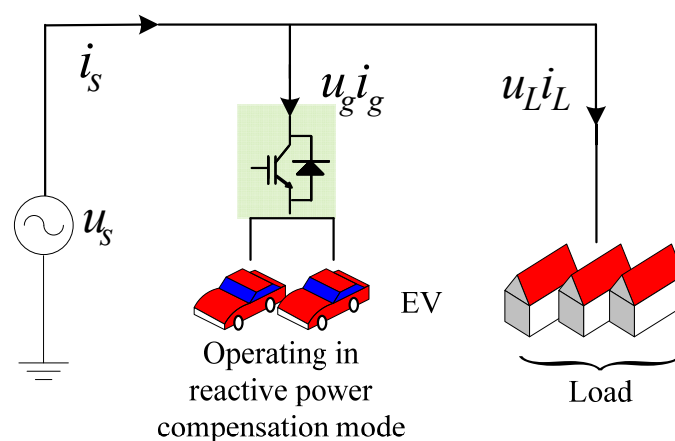


Figure 5. Simplified model of the household single-phase power supply system.

According to the characteristics of the proposed V2G topology, in reactive power compensation mode, the battery-side converter is a boost converter and the grid-side converter is a reactive power compensator. With the resistance-inductor load, the equivalent circuit and its phase diagram are shown in Figure 6. It is obvious that the grid-side voltage u_s and current i_s are approximately in phase.

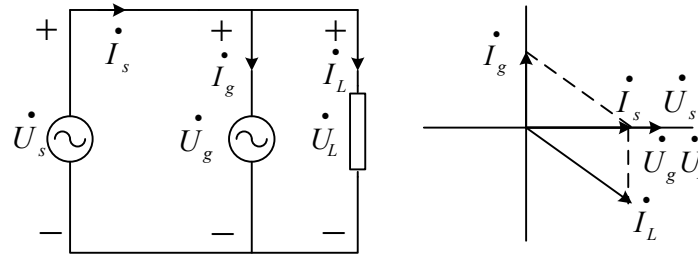


Figure 6. Equivalent circuit and vector diagram for EV system connected to an inductive load.

2.3.1. The Control Scheme of the Battery-Side Converter

For a single phase power system, the detection of instantaneous power is the key to reactive power compensation. Based on the p - q detection principle of three-phase instantaneous reactive power theory, the real-time detection of the harmonic and reactive current of a single-phase circuit is presented by constructing a virtual three-phase system to calculate the instantaneous power.

Using the grid-side voltage u_s and load-side current i_L in Figure 6, the three-phase grid-side voltage (u_{sa}, u_{sb}, u_{sc}) and three-phase load-side current (i_{La}, i_{Lb}, i_{Lc}) are obtained by phase-shifting and thus constructing a virtual symmetric three-phase system. According to the α - β coordinate transformation, the following two equations can be derived:

$$\begin{bmatrix} u_\alpha \\ u_\beta \end{bmatrix} = \sqrt{\frac{2}{3}} \begin{bmatrix} 1 & -1/2 & -1/2 \\ 0 & \sqrt{3}/2 & -\sqrt{3}/2 \end{bmatrix} \begin{bmatrix} u_{sa} \\ u_{sb} \\ u_{sc} \end{bmatrix} \tag{2}$$

$$\begin{bmatrix} i_\alpha \\ i_\beta \end{bmatrix} = \sqrt{\frac{2}{3}} \begin{bmatrix} 1 & -1/2 & -1/2 \\ 0 & \sqrt{3}/2 & -\sqrt{3}/2 \end{bmatrix} \begin{bmatrix} i_{La} \\ i_{Lb} \\ i_{Lc} \end{bmatrix} \tag{3}$$

Given the distortion and dynamic of grid voltage, i_p - i_q current detection method is introduced. Three-phase instantaneous active power p and instantaneous reactive power q are written as follows:

$$\begin{bmatrix} p \\ q \end{bmatrix} = \begin{bmatrix} u_\alpha & u_\beta \\ -u_\beta & u_\alpha \end{bmatrix} \begin{bmatrix} i_\alpha \\ i_\beta \end{bmatrix} \tag{4}$$

Then, the three-phase instantaneous active current i_p and instantaneous reactive current i_q are derived:

$$\begin{cases} i_p = \frac{u_\alpha}{u_\alpha^2 + u_\beta^2} p + \frac{u_\beta}{u_\alpha^2 + u_\beta^2} q \\ i_q = \frac{u_\beta}{u_\alpha^2 + u_\beta^2} p - \frac{u_\alpha}{u_\alpha^2 + u_\beta^2} q \end{cases} \tag{5}$$

2.3.2. System Configuration and Control Strategy

According to the principle of reactive power compensation, EVs must compensate all the reactive power of loads to make sure the grid-side voltage u_s and current i_s are approximately in phase. To ensure

that the grid-side current i_s only contains the load active power component i_p , the real-time detection current i_q should be given according to the current of EV-side. This given current on the EV-side can be used as a function which includes the active power component i_p . In this way, the given EV-side current is a variable which can be detected in real time. However, it is difficult to achieve accurate and stable control using ordinary PI.

On the other hand, the deadbeat control, which has superior dynamic performance, is based on accurate mathematical models. It uses state equations and output feedback signals to calculate the PWM signals of the next switch cycle. In Figure 7, ignoring the filter capacitor current, the equation of time domain in rectifying mode can be written as follows:

$$u'_g(t) = L_g \frac{di_g(t)}{dt} + u_s(t) \tag{6}$$

Within a sampling period T_s , transform above equation into:

$$\overline{u'_g}(k) = \frac{L_g}{T_s} [i_g(k+1) - i_g(k)] + \overline{u_s}(k) \tag{7}$$

where L_g is the filter inductor of grid converter side, $i_g(k)$ is the grid-side converter current at present sampling instant, $i_g(k+1)$ is the grid-side converter current at next sampling instant, $\overline{u'_g}(k)$ is the average of the converter output voltage, and $\overline{u_s}(k)$ is the average of the grid output voltage.

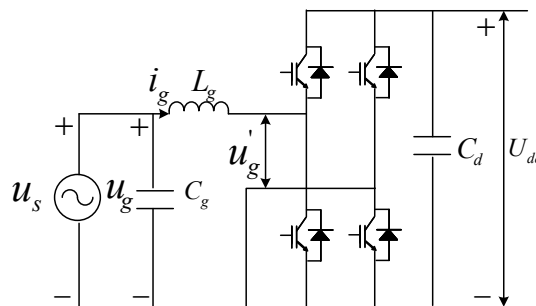


Figure 7. The circuit topology of grid-side.

To make the grid-side converter current i_g track the reference current $i_{ref}(k+1)$ at next sampling instant, $i_{ref}(k+1)$ is used to replace $i_g(k+1)$. Then, the converter duty cycle can be derived as:

$$D(k) = \frac{\overline{u'_g}(k)}{u_{dc}} = \frac{\frac{L_g}{T_s} [i_{ref}(k+1) - i_g(k)] + \overline{u_s}(k)}{u_{dc}} \tag{8}$$

Therefore, the reference current control is transformed into the converter duty control. Together with the detection of instantaneous power, the control frame of V2G grid-side converter for instantaneous power compensation is shown in Figure 8.

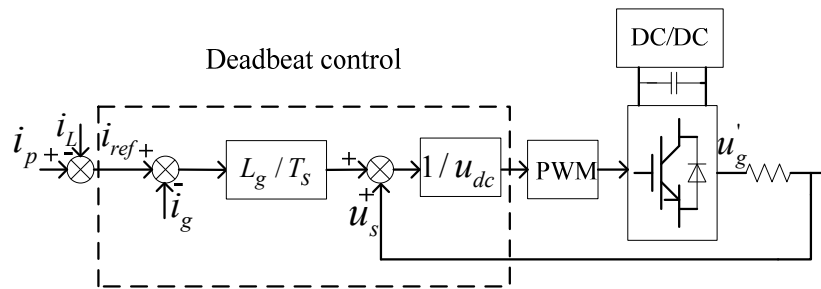


Figure 8. Control frame of system grid-side converter.

In Figure 8, when the system is steady, $i_g = i_{ref}$. Then $i_p - i_L = i_g$. According to Figure 8, $i_s = i_g + i_L = i_p$. This means that the grid-side current only contains the active component of the load current. Furthermore, since the active current component i_p passes through a low-pass filter, the high-order harmonics of the grid current can be eliminated. DC bus voltage is obtained from the battery-side boost converter. Therefore, its control strategy is same with that shown in Figure 3.

3. Simulation Results

This simulation is built upon a 4 kVA household charger with 400 V DC bus voltage and 220 V AC input voltage. The specifications of the designed procedure in this proposed circuit are listed in Table 1.

Table 1. The component values for proposed circuit.

Components	Symbols	Values
AC filter inductor	L_g	1.5 mH
AC filter capacitor	C_g	50 μ F/400 V
Discharged resistance	R	20 Ω /50 W
DC bus capacitor	C_d	2200 μ F/450 V
DC filter inductor	L_b	3 mH
DC filter capacitor	C_b	2200 μ F/450 V

3.1. The Simulation of Charge and Grid-Connected

The output current waveform on the grid-side under the emulated 220 V (RMS) grid voltage in charging mode is shown in Figure 9. At the beginning of the simulation, the load resistance is 10 Ω . The load variation is set at 1 s. A resistance whose value is 20 Ω is added to the original load in parallel. The battery is supplied with 4 kVA at full load. The output current of grid-side is sinusoidal and the power factor is approximately 1. The efficiency in this operating mode is about 85%. This makes the phase and frequency synchronize with the grid voltage very well. As represented in Figure 10, the THDs of the grid current are only 2.28% and 2.89% before and after the load changes, meeting the requirements of the IEEE standard 1547.

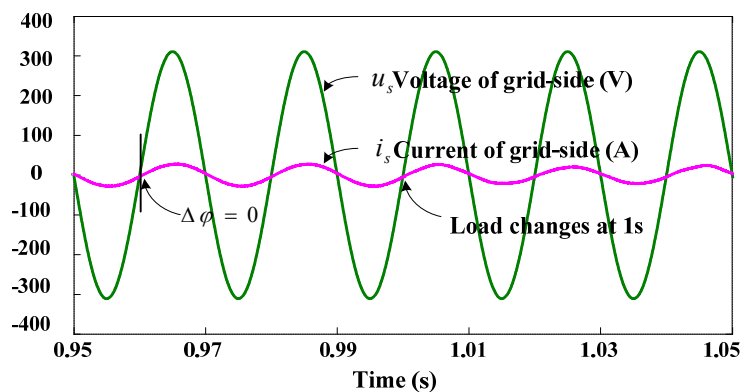


Figure 9. Control frame of system grid side converter.

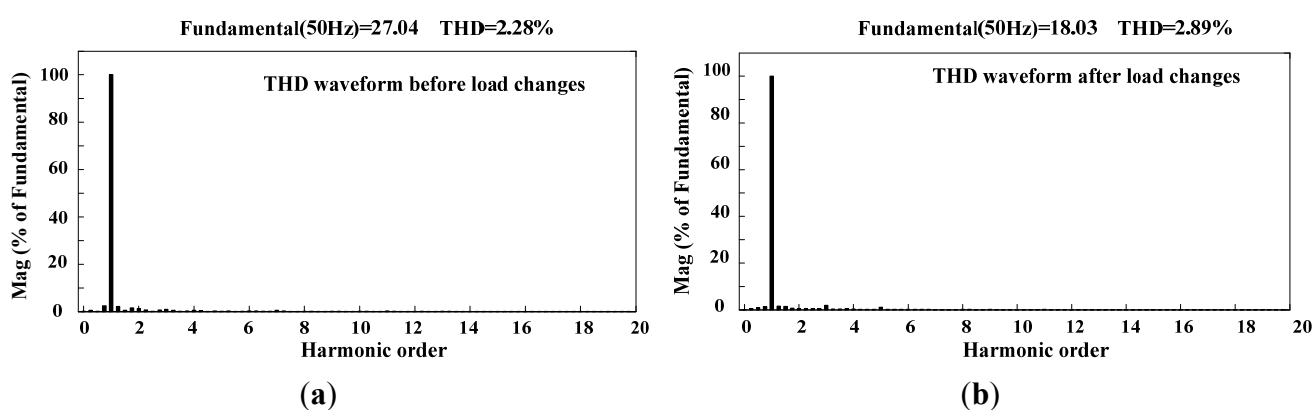


Figure 10. Control frame of system grid side converter. (a) Before load changes; (b) After load changes.

With the proposed control strategy, Figure 11 illustrates the response and stabilization at its initial setting value when a transient impedance change of battery charging is introduced. The output current maintains 20 A in CC charging mode and in the same way, the output voltage can retain 200 V in CV charging mode while the load changes at 1s. The dynamic response time in CC and CV charging is about 0.18 s. Therefore, the proposed circuit topology combined with the selected control strategy demonstrates its superiority in the charging mode.

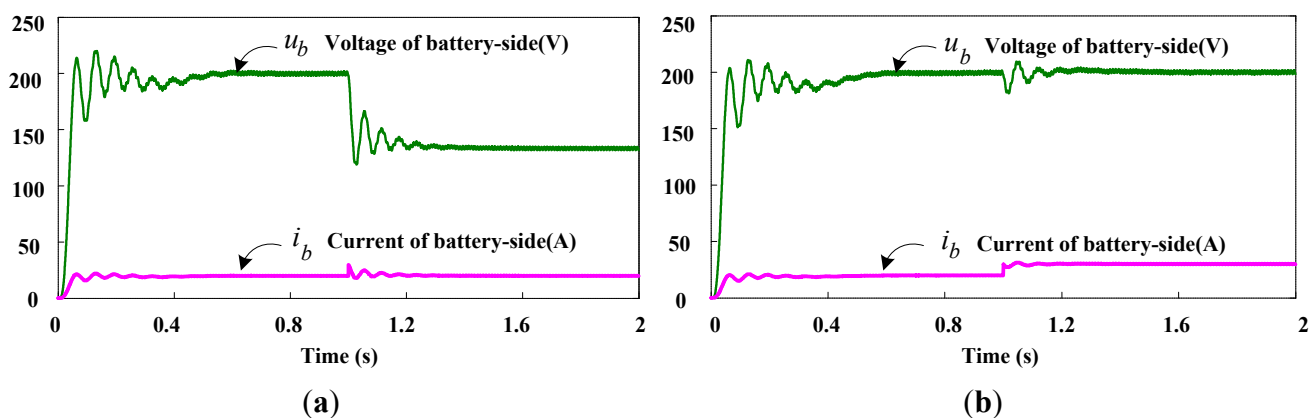


Figure 11. Output Simulated waveforms of battery-side. (a) Constant current charging mode; (b) Constant voltage charging mode.

Figure 12a shows the simulated input current and the grid voltage in grid-connected mode. It is worth noting that the input current is sinusoidal and an out-of-phase current is generated here. The phase of the grid-connected current is opposite with the grid voltage phase at full active operation. Therefore, the results are consistent with the design requirements. The efficiency in grid-connected operating mode is about 87% and the THD of the input current is only 1.98% in Figure 12b. This is much lower than 5% and can meet the requirements of IEEE 1547. Thus, the PR control strategy under selection can result in outstanding performance in grid-connected mode.

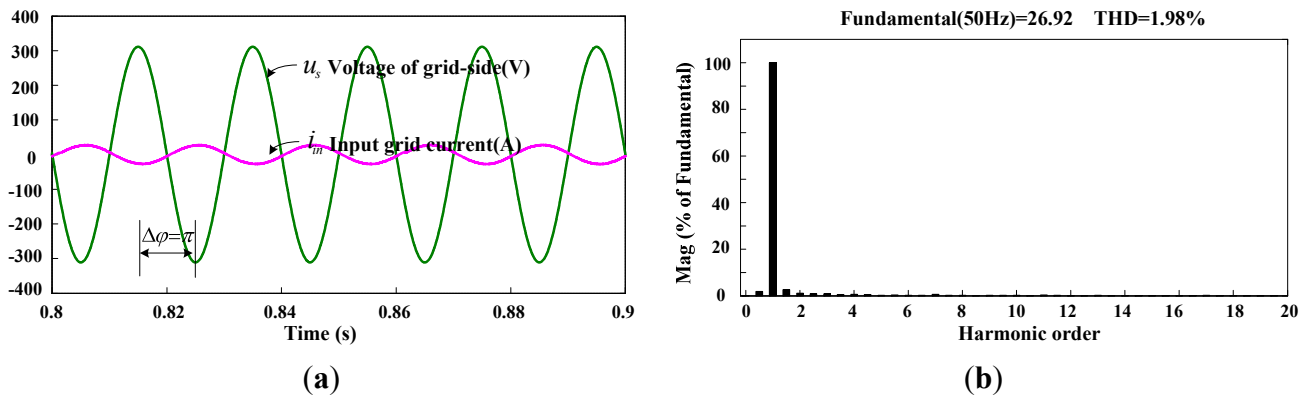


Figure 12. (a) Input grid current and grid voltage in grid-connected mode; (b) THD waveform of the input grid current in grid-connected mode.

3.2. The Simulation of Reactive Power Compensation

In reactive power compensation mode, a resistance-inductor load is employed to verify the capacity of the reactive power compensation, where the inductor is 0.05 H and the resistance is 20 Ω . The simulation results are shown in Figures 13 and 14. As shown in Figure 13, the electric vehicle access achieves a good compensation for local loads, and the current response curve is very smooth and sinusoidal. From Figure 14, it is seen that the voltage’s phase lags the current’s by 90° and the electric vehicle is operating in reactive power compensation mode.

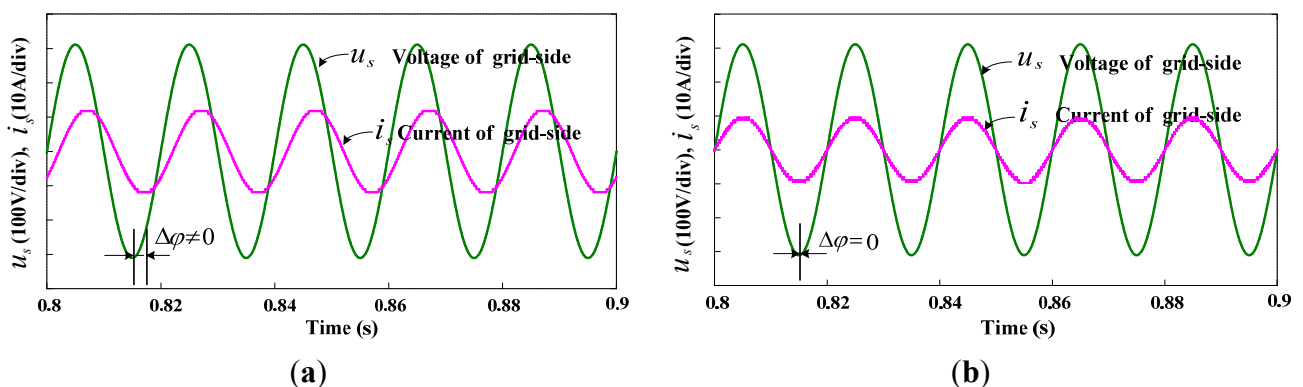


Figure 13. The voltage and current waveforms of grid-side in reactive compensation mode. (a) Before compensation; (b) After compensation.

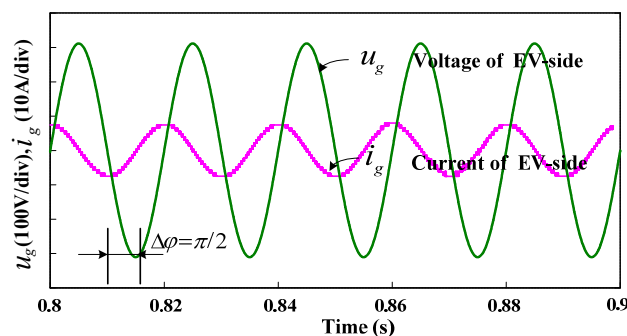


Figure 14. The voltage and current waveforms of the EV-side.

4. Experimental Results

Finally, the proposed control schemes are verified experimentally. The experimental equipment mainly includes a power stage with dual SKM 50 GB 123D IGBT modules and a digital signal processor (DSP) card based on Texas Instrument's DSP chip TMS320F28335. Considering the realistic conditions and lab safety, the system we use can provide 1 kVA to the battery charger, grid-connected, or reactive power compensation.

4.1. Charging Mode Experiment

Based on the charging mode experiment, the constant voltage charging mode and current charging mode have been studied in this section. The experimental parameters of the proposed circuit and control system are described below. The experimental power is 500 W, with 110 V (RMS) AC input voltage on the grid-side and 200 V DC bus voltage. Meanwhile, the setting constant voltage output is 100 V and the current is 4 A. The load on the EV-side will be instead set by a resistance whose value is 30 Ω . Considering the limitations of the converter, the switching frequency is set to 10 kHz.

Figure 15 shows the voltage and current waveforms in CC and CV charging mode with the PR controller. It can be noted that the output current working in CC charging mode maintains 4 A and the output voltage can maintain nearly 100 V to perform CV charging mode. It can realize constant current and constant voltage with ideal waveforms. The experiment indicates that the frequency of the current and voltage in the grid-side are almost identical. The phase as well as the frequency of output current can nearly keep pace with those of the grid voltage, which proves the control performance and the single phase PLL.

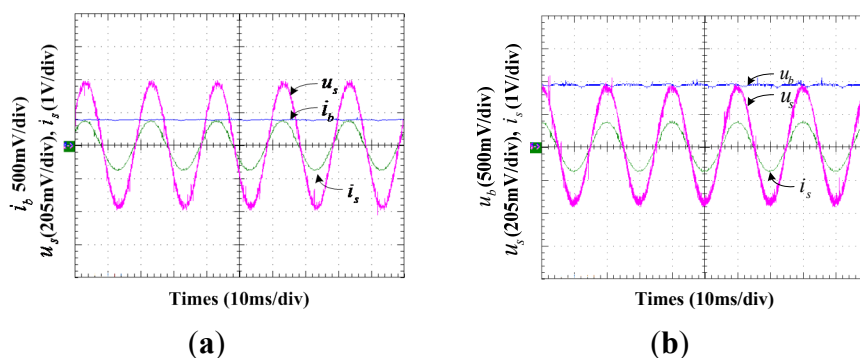


Figure 15. The voltage and current in charging mode. (a) Constant current charging mode; (b) Constant voltage charging mode.

4.2. Grid-Connected Mode Experiment

Considering the experimental conditions, the experimental parameters of the the proposed circuit and control system is modified as follows: the constant voltage output setting is 100 V and the maximum output current is 5 A. The battery of the EV-side will be instead represented by a 110 V/10 A DC power source. The output AC voltage of the grid-side is 70 V (RMS) and the grid-connected current is 10 A (p-p). The DC bus voltage is 150 V. The switching frequency of the converter is as same as it was in the charging mode experiment.

Figure 16 shows the voltage and input current waveforms in the grid-connected mode. The output grid-side current is sinusoidal, of which the phase remains opposite the grid voltage for the unchanged connection. The requirement results and emulations are basically the same. Therefore, the bi-direction EV system can achieve high performance with the proposed control strategy.

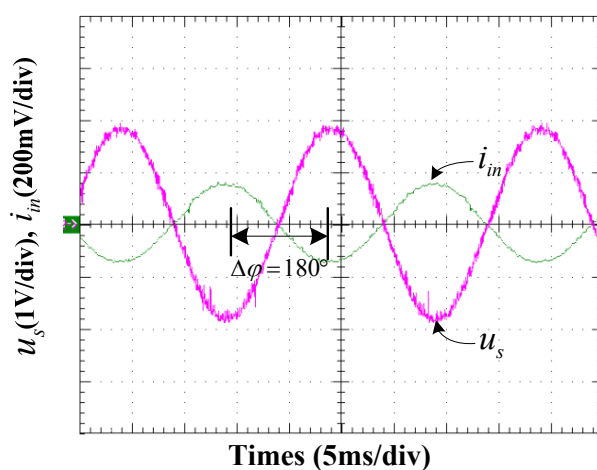


Figure 16. The voltage and current in grid-connected mode.

4.3. Reactive Power Compensation Mode Experiment

In order to verify the good reactive compensation performance of the control strategy, the results were checked by the experiments described below. The load of the EV-side will be instead represented by a resistive and inductive load. The value of the resistance is 14 Ω and the inductance is 0.012 H. Being restricted by the experimental environment and practical conditions as well, the voltage of the grid side is 40 V (RMS) and the battery side is 48 V. The DC bus voltage is 100 V. The experimental waveforms are as follows.

Figure 17 shows the grid voltage and current waveforms before and after compensation. The system functions as active power current source and the unit power factor are acquired. With respect to Figure 17, the current waveform is smooth and sinusoidal thanks to the EV's compensation.

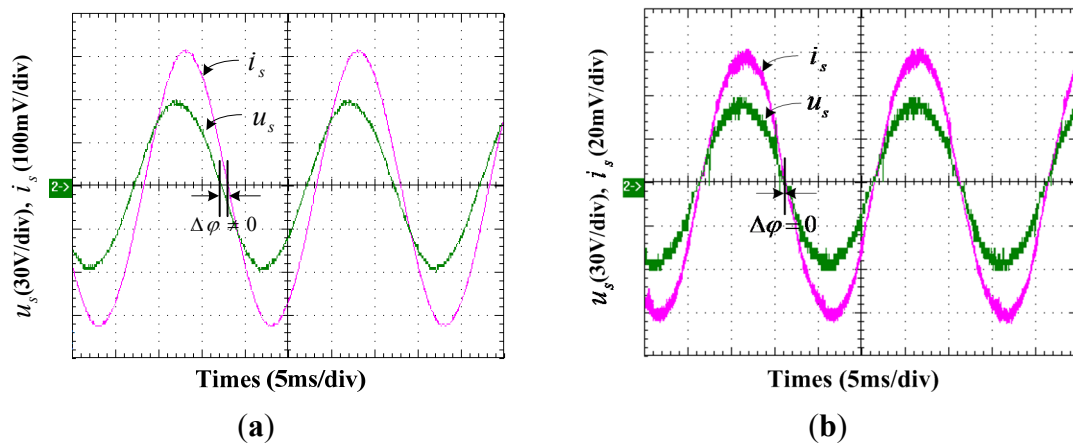


Figure 17. The voltage and current in reactive power compensation mode. (a) Before compensation; (b) After compensation.

5. Conclusions

This paper presents a new multi-function conversion technique for vehicle-to-grid (V2G), including bi-directional convert topology, control strategy and reactive compensation application based on V2G. A circuit topology including a protection unit for V2G based on the household electric system in China is presented. Based on the circuit, an integrated control strategy for V2G energy bi-directional transfer which consists of a battery-side controller and a grid-side controller is studied. In order to improve the whole system performance, a proportional-resonant (PR) control is applied. Furthermore, the control scheme of V2G for reactive power compensation is analyzed. A control scheme combined with instantaneous reactive power detection methods and deadbeat control is employed. Finally, simulations and experiments are carried out to verify the feasibility of the proposed circuit and control scheme. The simulation and experimental results show that the design system can perform well in multi-function conversion including V2G energy bi-directional transformation and reactive power compensation.

Acknowledgments

This work was supported in part by the NSFC under Projects 51177012 and 61374125, the 973 Program of China under Project 2013CB035603.

Author Contributions

The manuscript is a part of the master thesis of Zhongbing Xue and jointly supervised by Ying Fan, Department of Electrical Engineering, Southeast University. The design and analyses, as well as the experiments were carried out by Zhongbing Xue under support of Li Zhang and Zhixiang Zou. In addition, the manuscript was improved and revised by Weixia Zhu.

Conflicts of Interest

The authors declare no conflict of interest.

References

1. Dickerman, L.; Harrison, J. A New Car, a New Grid. *IEEE Power Energy Mag.* **2010**, *8*, 55–61.
2. Zheng, P.; Tong, C.; Bai, J. Magnetic Decoupling Design and Experimental Validation of a Radial-Radial Flux Compound-Structure Permanent-Magnet Synchronous Machine for HEVs. *Energies* **2012**, *5*, 4027–4039.
3. Song, Y.; Yang, Y.; Hu, Z. Present Status and Development Trend of Batteries for Electric Vehicles. *Power Syst. Tech.* **2011**, *35*, 1–7.
4. Landi, M.; Gross, G. Measurement Techniques for Online Battery State of Health Estimation in Vehicle-to-Grid Applications. *IEEE Trans. Instrum. Meas.* **2014**, *63*, 1224–1234.
5. Peña, Y.K.; Nieves, J.C.; Espinoza, A.; Borges, C.E.; Pena, A.; Ortega, M. Distributed Semantic Architecture for Smart Grids. *Energies* **2012**, *5*, 4824–4843.
6. Yilmaz, M.; Krein, P.T. Review of the Impact of Vehicle-to-Grid Technologies on Distribution Systems and Utility Interfaces. *IEEE Trans. Power Electron.* **2013**, *28*, 5673–5689.
7. Ehsani, M.; Falahi, M.; Lotfifard, S. Vehicle to Grid Services: Potential and Applications. *Energies* **2012**, *5*, 4076–4090.
8. Liu, C.; Chau, K.T.; Wu, D.; Gao, S. Opportunities and Challenges of Vehicle-to-Home, Vehicle-to-Vehicle, and Vehicle-to-Grid Technologies. *Proc. IEEE* **2013**, *101*, 2409–2427.
9. Chau, K.T.; Chan, C.C. Emerging Energy-Efficient Technologies for Hybrid Electric Vehicles. *Proc. IEEE* **2007**, *95*, 821–835.
10. Clement-Nyns, K.; Haesen, E.; Driesen, J. The impact of charging plug-in hybrid electric vehicles on a residential distribution grid. *IEEE Trans. Power Syst.* **2010**, *25*, 371–380.
11. Clement-Nyns, K.; Haesen, E.; Driesen, J. The impact of vehicle-to-grid on the distribution grid. *Electric Power Syst. Res.* **2011**, *81*, 185–192.
12. Lassila, J.; Haakana, J.; Tikka, V.; Partanen, J. Methodology to Analyze the Economic Effects of Electric Cars as Energy Storages. *IEEE Trans. Smart Grid* **2012**, *3*, 506–516.
13. Fan, Y.; Zhang, L.; Xue, Z.; Zou, Z. Reactive Compensation Technology Based on Vehicle-to-Grid. *Power Syst. Tech.* **2013**, *37*, 307–311.
14. Jiang, J.; Bao, Y.; Wang, L. Topology of a Bidirectional Converter for Energy Interaction between Electric Vehicles and the Grid. *Energies* **2014**, *7*, 4858–4894.
15. Yu, Y.; Zhang, Q.; Liang, B.; Liu, X.; Cui, S. Analysis of a single-phase Z-source inverter for battery discharging in vehicle to grid applications. *Energies* **2011**, *4*, 2224–2235.
16. Su, M.; Wang, H.; Sun, Y.; Yang, J.; Xiong, W.; Liu, Y. AC/DC Matrix Converter with an Optimized Modulation Strategy for V2G Applications. *IEEE Trans. Power Electron.* **2013**, *28*, 5736–5745.
17. He, Y.; Venkatesh, B.; Guan, L. Optimal Scheduling for Charging and Discharging of Electric Vehicles. *IEEE Trans. Smart Grid* **2012**, *3*, 1095–1105.
18. Jin, C.; Tang, J.; Ghosh, P. Optimizing Electric Vehicle Charging With Energy Storage in the Electricity Market. *IEEE Trans. Smart Grid* **2013**, *4*, 311–320.
19. Liu, H.; Hu, Z.; Song, Y.; Lin, J. Decentralized vehicle-to-grid control for primary frequency regulation considering charging demands. *IEEE Trans. Power Syst.* **2013**, *28*, 3480–3489.
20. Ustun, T.; Ozansoy, C.; Zayegh, A. Implementing Vehicle-to-Grid (V2G) Technology with IEC 61850-7-420. *IEEE Trans. Smart Grid* **2013**, *4*, 1180–1187.

21. Long, B.; Ryu, J.H.; Lim, S.T.; Chong, K.T. Design and Control of a Multi-Functional Energy Recovery Power Accumulator Battery Pack Testing System for Electric Vehicles. *Energies* **2014**, *7*, 1376–1392.
22. Kisacikoglu, M.C.; Ozpineci, B.; Tolbert, L.M. Effects of V2G Reactive Power Compensation on the Component Selection in an EV or PHEV Bidirectional Charger. In Proceedings of the IEEE Energy Conversion Congress and Exposition, Delft, The Netherlands, 25–27 August 2010; pp. 870–876.
23. Kisacikoglu, M.C.; Ozpineci, B.; Tolbert, L.M.; Wang, F. Single-phase inverter design for V2G reactive power compensation. In Proceedings of the IEEE Applied Power Electronics Conference, Fort Worth, TX, USA, 6–11 March 2011; pp. 808–814.

© 2015 by the authors; licensee MDPI, Basel, Switzerland. This article is an open access article distributed under the terms and conditions of the Creative Commons Attribution license (<http://creativecommons.org/licenses/by/4.0/>).